Physical measurements of the backward erosion piping process

B.A. Robbins
U.S. Army Engineer Research and Development Center

V.M. van Beek
Deltares

Abstract: A novel laboratory device is presented, in which the process of backward erosion piping is observed in cylindrical sand samples oriented horizontally. The cylindrical shape of the testing device constrained the location of the erosion path to the top of the sample, thereby allowing pore pressure measurements to be made in both the eroded pipe and the surrounding soil. Additionally, the pipe depth and width were measured. From the measurements, the local hydraulic gradient upstream of the pipe tip and the critical shear stress in the bottom of the eroded pipe were calculated. Results indicate that the local critical hydraulic gradient measured over a distance of 10 cm upstream of the pipe is not influenced by experiment scale. Further, the measurements suggest that the sediment transport in the eroded pipe can be adequately modelled using classic sediment transport theory for open channel flow.

Keywords: piping, backward erosion, seepage.

1 INTRODUCTION

Backward erosion piping (BEP) refers to a process by which sand is gradually eroded from the foundation of dams and levees. Erosion initiates at the downstream side of a structure where unfiltered seepage exits the foundation. The erosion then progresses upstream through sandy foundation material along the contact with a cohesive cover layer. The eroded materials are transported through the developing erosion channels towards the unfiltered seepage exit where they are deposited on the ground surface in a cone of sand (sand boil). If allowed to progress, the erosion channels may eventually connect to the river or reservoir upon which rapid enlargement of the erosion channels occur, possibly leading to catastrophic failure of the overlying embankment. For detailed descriptions of the process and physics of BEP, the interested reader is referred to Van Beek (2015).

BEP has been shown to account for approximately one-third of all internal erosion related failure modes (Richards and Reddy, 2007). Further, visible evidence of BEP activity is observed along levees during relatively frequent flood events (Turnbull and Mansur, 1961; USACE, 1956; ENW, 2010). As such, BEP has been the subject of numerous studies (Schmertmann, 2000; Sellmeijer, 1988; Townsend et al., 1981; Van Beek et al., 2011). Many of these studies were experimental in nature and attempted to measure the overall hydraulic conditions causing erosion to develop upstream. Typically, experiments of this nature are conducted in rectangular boxes in which a sand sample is subjected to unidirectional, horizontal flow. Erosion initiates at the downstream end of the sample and is allowed to progress along the sample boundary until it reaches the upstream end of the sample. Because of the rectangular shape of the sample, the erosion channels typically meander along the sample boundary seeking out the path of least resistance. In the case of the meandering channels, the location of the channel is not known *a priori* but rather varies from test to test. Therefore, it is typically not possible to make detailed measurements of the local hydraulic conditions near the developing erosion front. For this reason, the critical hydraulic gradient causing erosion is often characterized by the average hydraulic gradient across the sample. Using this average measurement to characterize the behavior requires that the measurements be adjusted

for geometry, scale, and boundary conditions to be applied to other conditions, such as the field (Schmertmann, 2000; Sellmeijer et al., 2011). In this study, a novel laboratory device is presented that permitted local measurements of the hydraulic aspects of the BEP process. From these measurements, insights are obtained regarding local hydraulic conditions causing pipe progression and flow conditions in the eroded pipes.

2 LABORATORY TESTING

In the following sections, the laboratory device, test procedures, and characteristics of the sand used for testing are briefly described. Detailed descriptions are available in Robbins et al. (2017).

2.1 Equipment

The laboratory equipment for the experiments presented in this paper consists of two acrylic cylinders fitted with pressure transducers along the top and bottom as shown in Figure 2.1. The two cylinders were identical in all regards except for diameter (D). One cylinder had an internal diameter of 76.2 mm (Tube B), and the other cylinder had a diameter of 152.4 mm (Tube C). The two cylinder sizes were constructed to allow for the investigation of scale effects.

The cylinder is fixed to a rotating frame, such that the sand can be placed into the cylinder through water pluviation while in the vertical position. The cylinder is then rotated to the horizontal position for testing, causing the sand to form a natural slope at the downstream end of the tube. Eleven pressure transducers were located along the top and bottom of the sample at 0.1-m intervals. The head applied to both the upstream and downstream boundaries was regulated through constant head, overflow tanks. The downstream head tank was fixed, whereas the upstream head tank was raised through a winch and pulley system. In this manner, the upstream head could be controlled to the nearest millimeter. The pressure transducers were connected to a USB data acquisition module so that measurements could be recorded at one-second intervals. The flow rate was also recorded at one-second intervals by capturing the outflow in a bucket connected to a load cell with a resolution of 1 gram. In this manner, the outflow could be measured to the nearest mL/sec.

The cylindrical shape and the sloping sand bed resulted in the shortest seepage path (and highest gradients) occurring at the top (center) of the sample. Because of this, erosion would initiate at the top of the slope and progress backward along the sample directly beneath the pressure transducers. In this manner, detailed pressure measurements were recorded in the soil and eroded pipe during the process of BEP.

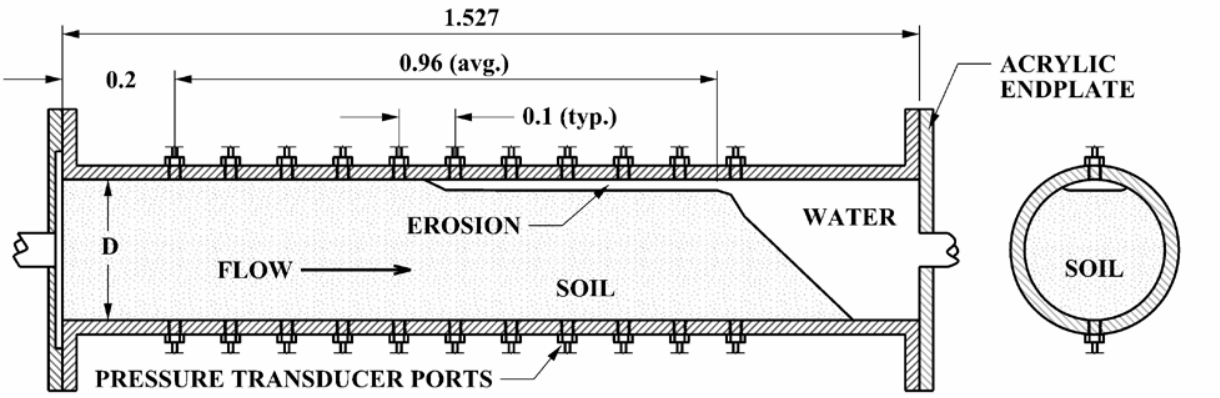

Figure 2.1. Schematic diagram of the laboratory testing device (units of meters).

2.2 Procedures

The following test procedures were followed for all tests conducted in this study.

1. The device was rotated to a vertical position for sample placement and saturated with deaired water.
2. The sand was water pluviated into the device from the top, tapping the sides of the cylinder with a rubber mallet during placement to achieve differing levels of densification.
3. After the sample was placed, the device was rotated to the horizontal position. The downstream slope would develop during rotation, coming to rest at the sand's natural angle of repose.
4. The upstream head tank was incrementally raised to increase the average gradient across the sample. The increments were selected to cause changes in average gradient varying from 0.01 to 0.05, with larger increments used during the beginning of the test. As critical conditions were approached, head increments resulting in gradient changes of 0.01 were used exclusively. In this manner, the hydraulic conditions at the onset of piping could be precisely measured.
5. Once piping initiated, the pipe was allowed to progress through the sample with pressure measurements and flow rate measurements being recorded at a frequency of 1 Hz. In some cases, the head was decreased once the pipe progressed halfway through the sample to stop the erosion. Once the erosion was stopped, the upstream head was gradually increased again until erosion was observed. This allowed the local hydraulic gradient near the head of the pipe to be measured at the onset of piping. When erosion reinitiated, it was allowed to progress the remainder of the way through the sample.
6. After the pipe progressed entirely through the sample, the pipe channel was allowed to enlarge until the sand in the bottom of the pipe came into equilibrium (as indicated by minimal grain movements). Measurements of the channel dimensions, pressure gradient, flow rate, and maximum flow velocity in the pipe (as indicated by colored dye streams) were obtained at the equilibrium state. These measurements were also recorded in some instances when the pipe was stopped part way through the sample.

2.3 Materials

A single sand was used for testing in both Tube B and Tube C. The sand, referred to as 40/70 sand, falls predominantly between the No. 40 and No. 70 U.S. sieve sizes. The sand characteristics are presented in Table 1. ASTM testing standards D4253 and D4254 were used to determine the maximum and minimum void ratios.

Table 1. Characteristics of 40/70 Sand

Property	Value
d_{10} (*mm*)	0.227
d_{30} (*mm*)	0.268
d_{60} (*mm*)	0.322
C_c	0.98
C_u	1.42
e_{min}	0.56
e_{max}	0.80
Specific gravity	2.65

2.4 Test Results

A total of 11 tests were conducted: 7 tests in Tube B and 4 tests in Tube C. For each test, the average critical gradient across the sample for BEP initiation was recorded at the moment of pipe initiation. The critical average gradients obtained for all tests are shown in Figure 2.2. For all tests, a general decrease in

critical gradient with increasing void ratio is observed. This trend corresponds well with the results of previous studies (Van Beek et al., 2009; Weijers and Sellmeijer, 1993). Further, the tests conducted in Tube C exhibit lower average critical gradients than the tests in Tube B due to scale effects (Van Beek, 2015; Schmertmann, 2000). As the tube diameters are sufficiently different for scale effects to be exhibited, the experiment results can be examined at a local scale to determine if local hydraulic measurements are also subject to scale effects.

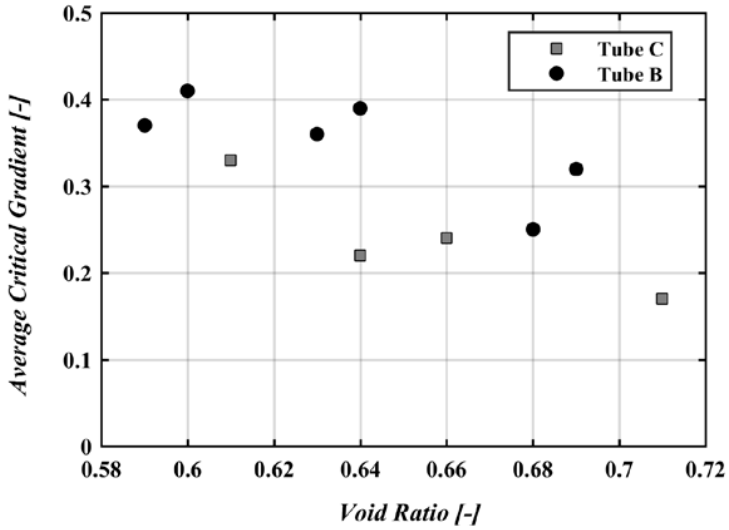

Figure 2.2. Average gradient measured at initiation of piping for all tests.

During each test, as the pipe passed the pressure transducers, the local horizontal gradient (over 10 cm) along the top of the sample was measured between each pair of pressure transducers. Additionally, the local vertical gradient (across the diameter of the cylinder) was measured across each pair of top/bottom transducers. Whenever the pipe reached a pressure transducer, the local horizontal gradient measured over the 10 cm immediately upstream of the pipe head obtained its maximum value. Likewise, the local vertical gradient measured at the location of the pipe head also reached its maximum value. Each time the pipe passed a pressure transducer, the magnitude of the maximum horizontal and vertical local gradients was noted. The measured values are shown in Figure 2.3. In most instances, the pipe was actively progressing as it passed the transducers and showed no signs of being near the critical conditions for progression. However, in a few instances (typically after the stopped pipe was restarted) the conditions were nearly at equilibrium and the pipe would stop progressing momentarily at the transducer location. The local gradients measured under these equilibrium conditions are distinguished in Figure 2.3.

Important observations that advance the understanding of BEP were made from the results of this testing. First, local measurements of gradient were substantially higher than the average gradients. This is indicative of the concentration in flow and high gradients that occur in the vicinity of the pipe head (Vandenboer et al., 2014) . Secondly, it should be noted that the majority of the local gradient measurements were significantly larger than the critical, local gradient values measured near equilibrium. This can be explained by the fact that BEP is controlled by initiation in small experiments with sloped exits (Van Beek et al., 2014). That is, for this experiment configuration once BEP initiates, it will progress continuously through the sample due to the critical gradient for progression being far exceeded. This observation is confirmed by the generally high values of local horizontal gradient for the majority of the measurements. Lastly, the local critical gradients measured at the verge of equilibrium (Figure 2.3) are nearly identical in magnitude for both tube diameters and appear to be independent of the vertical gradient. This suggests that, when measured over a small enough distance, a scale-independent critical gradient can be measured. Further, it is solely the horizontal component of this local gradient that appears to control the progression of BEP.

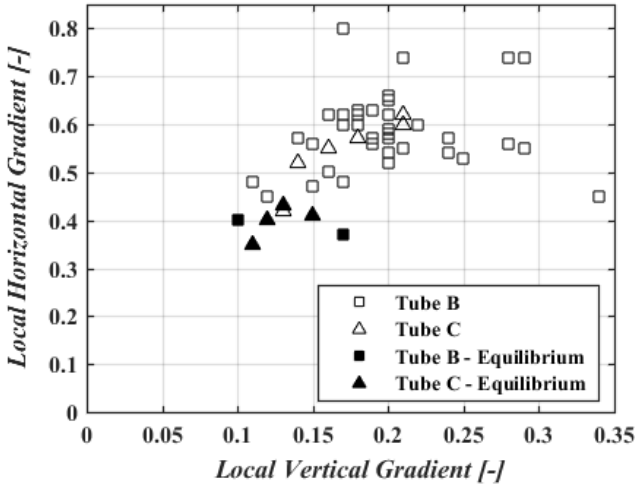

Figure 2.3. Local gradient measurements obtained during pipe progression.

3 PIPE CHANNEL EROSION

During each test, stable pipe channel configurations were obtained, in which the sand particles in the bottom of the pipe were in equilibrium. In some cases, stable pipe channels were obtained with the pipe penetrating through only a fraction of the sample. When stable pipe channel sections were obtained, the channel dimensions, pressure gradient, and maximum flow velocity were obtained as previously discussed. Approximating the pipe channel cross section as an ellipse, the channel wall shear stress, τ_w (N/m^2), can be computed from the measured quantities for laminar flow conditions (Van Beek et al, 2017) by

$$\tau_w = \sqrt{\rho_w g \frac{\partial \varphi}{\partial x} v_{\max} 2\mu} \tag{1}$$

where ρ_w (kg/m^3), g (m/s^2), $\partial\phi/\partial x$, v_{max} (m/s), and μ (Ns/m^2) represent the fluid density, acceleration of gravity, hydraulic gradient in the pipe channel, maximum flow velocity in the pipe channel, and dynamic fluid viscosity, respectively. In all experiments, the flow was observed to be laminar as indicated by the smooth dye streamlines (Figure 3.1). If the wall shear stress exceeds the critical shear stress for sediment transport, the wall of the erosion channel is eroded and the pipe deepens. The depth of the erosion channel is a fundamental aspect of numerical computations of coupled seepage-pipe hydraulics (Sellmeijer, 2006; Van Esch et al., 2013), and indirectly influences the local gradient at the pipe tip as well. Because of the importance of the pipe depth in BEP hydraulic computations, it is imperative that the critical shear stress be known precisely. Current practice in the Netherlands (TAW, 1999) predicts the critical shear stress, τ_c (N/m^2), in piping calculations using the approach proposed by White (1940) where

$$\tau_c = \eta \frac{\pi}{6} \gamma_p' d \tan\theta \tag{2}$$

with η, γ_p' (N/m^3), d (m), and θ ($degrees$), denoting White's constant, the submerged particle specific weight, the particle diameter, and the bedding angle of the sand particles, respectively. The values of White's constant and bedding angle have been prescribed through calibration of numerical models to large scale experiments (Lopez de la Cruz, Calle, and Schweckendiek, 2011). Relying on a fixed-parameter set based on model calibration brings into question the validity of the model under conditions

outside the calibration data set. A more generic approach for predicting the critical shear stress in BEP pipes was proposed by Hoffmans (2014) using the Shields curve as applied to open channel sediment transport problems. The Shields curve relates the dimensionless particle Reynolds number, given by

$$\mathrm{Re}^* = \frac{\rho_w u^* d_{50}}{\mu} \text{ with } u^* = \sqrt{\frac{\tau_w}{\rho_w}} \tag{3}$$

to the Shields parameter given by

$$\Psi_c = \frac{\tau_c}{\gamma_p' d} = f\left(\frac{\rho_w u^* d}{\mu}\right) \tag{4}$$

The general relationship between the particle Reynolds number and the Shields parameter has been determined experimentally for a variety of sediments and flow conditions (ASCE, 2008). Using this relationship, the flow conditions in the pipe can be related to the critical shear stress of the sediments in the bottom of the pipe to adjust BEP models to a broad variety of conditions.

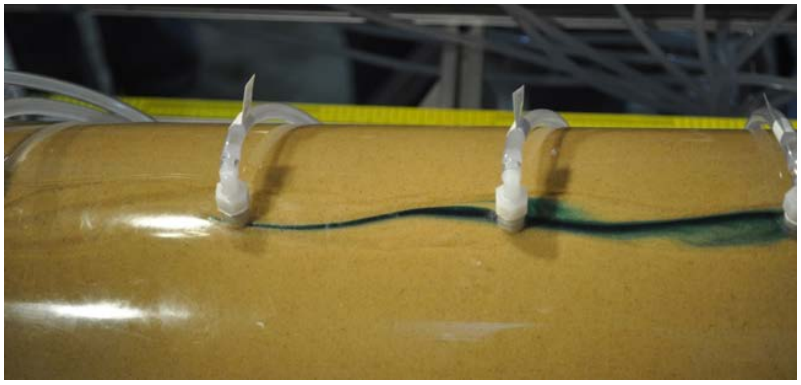

Figure 3.1. Stream lines indicative of laminar flow conditions in the developed pipes.

To examine the applicability of the Shields approach to BEP modeling, the erosion channel wall shear stress (shear stress exerted on the particles in the bottom of the pipe) was computed for all experiments in which the particles at the bottom of the eroded pipe appeared to be in equilibrium. Equilibrium was judged to be obtained when the pipe depth appeared to be constant and particle movement was relatively infrequent. The wall shear stress under these conditions was considered to be the critical shear stress of the sand particles, which relies on the observation by Govers (1987) that the transition from a stable to an unstable bed is sharply discernible in laminar flow as fluctuating shear stresses are absent. The wall shear stress for each experiment (both with the pipe penetrating partially and fully) was computed using Equation 1 with the measured pressure gradient and maximum velocity. The computed critical shear stress for the sand particles at the bottom of the BEP channels was compared to the Shields diagram (Cao, 2006) and various other data sets obtained in laminar flow conditions (Govers, 1987; Loiseleux et al. 2005; Mantz, 1977; C.M. White, 1940; S. White, 1970; Yalin and Karahan, 1979) as shown in Figure 3.2. Additionally, the Shields parameter corresponding to using White's approach with fixed parameters is shown on Figure 3.2 for comparison purposes. From the results, it is apparent that the Shields parameter estimated for the sediment in the BEP erosion channels corresponds well to both the data in the literature for laminar flow and the Shields curve. It is also interesting to note that the BEP data appears to be towards the upper end of the laminar flow regime, approaching the transition zone (near a particle Reynolds number of 10). For sands that are much coarser than those tested in this study, it is quite likely that the flow conditions will begin to become turbulent. This must be considered when applying the results of this study to BEP models.

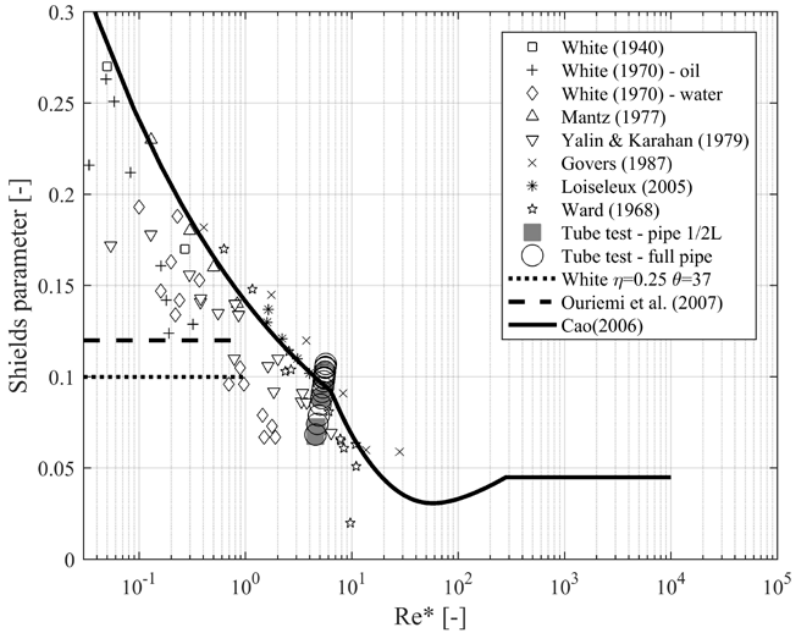

Figure 3.2. Shields parameter determined from laboratory experiments compared to data in the literature.

4 CONCLUSIONS

A cylindrical test device was constructed in which backward erosion piping (BEP) experiments could be conducted. The cylindrical sample shape ensured that the erosion path progressed along the center of the sample. Pore pressure transducers located along the top and bottom of the sample allowed the pressure gradients to be measured in the soil surrounding the pipe and in the pipe channel itself. From these measurements, it was found that the horizontal, hydraulic gradient measured over a distance of 10 cm in front of the advancing pipe was significantly higher than average hydraulic gradients across the entire sample. The local gradients were also, in the majority of cases, higher than the threshold gradient for progression. In instances where pipe progression was stopped, the local critical gradient in front of the advancing pipe was measured. It was found that the critical horizontal gradient 10 cm upstream of the pipe did not exhibit scale effects found in the average gradient measurements across the entire sample. Lastly, the gradient measurements obtained in the eroded pipe channels allowed the critical shear stress of the pipe sediments to be calculated. Results indicate that the incipient motion conditions in the pipe channel bottom align well with the Shields approach for predicting incipient motion. This validates the use of Shields diagram for BEP modeling providing a generic transport approach encompassing all conditions resulting in laminar flow. The combination of a local critical gradient in front of the pipe and the Shields approach for predicting incipient motion in the pipe allows for modeling of pipe progression.

Permission to publish was granted by Director, Geotechnical & Structures Laboratory.

REFERENCES

ASCE. (2008). *Sedimentation Engineering*. (M. Garcia, Ed.). American Society of Civil Engineers.

Cao, Z., Pender G., & Meng, J. (2006). Explicit Formulation of the Shields Diagram for Incipient Motion of Sediment. *Journal of Hydraulic Engineering*, October 2006: 1097-1099.

ENW (Expertisenetwerk Waterveiligheid) (2010) Piping – Realiteit of Rekenfout. Expertisenetwerk Waterveiligheid, see http://www.enwinfo.nl/upload/Piping%20-%20Realiteit%20of%20Rekenfout%20(72dpi).pdf (accessed 16-09-2013)

Govers, G. (1987). Initiation of motion in overland flow. *Sedimentology*, *34*(6), 1157–1164.

https://doi.org/10.1111/j.1365-3091.1987.tb00598.x
Hoffmans, G.J.C.M. (2014). An Overview of Piping Models. In *ICSE7* (p. 17). Perth, Australia.
Loiseleux, T., Gondret, P., Rabaud, M., & Doppler, D. (2005). Onset of erosion and avalanche for an inclined granular bed sheared by a continuous laminar flow. *Physics of Fluids*, *17*(10). https://doi.org/10.1063/1.2109747
Lopez de la Cruz, J., Calle, E., & Schweckendiek, T. (2011). Calibration of Piping Assessment Models in the Netherlands. In *International Symposium on Geotechnical Risk and Safety* (pp. 587–595). Munich, Germany. Retrieved from http://vzb.baw.de/digitale_bib/geotech2011/PDF/5 Flood Defence/5_04.pdf
Mantz, P.A. (1977). Incipient transport of fine grains and flakes by fluids - Extended Shields diagram. *J. Hydr. Div.*, *103*(HY6), 601–615.
Richards, K.S., & Reddy, K.R. (2007). Critical appraisal of piping phenomena in earth dams. *Bulletin of Engineering Geology and the Environment*, *66*(4), 381–402. https://doi.org/10.1007/s10064-007-0095-0
Robbins, B.A., van Beek, V.M., Lopez-Soto, J., Montalvo-Bartolomei, A., Murphy, J. (2017). A novel laboratory test for backward erosion piping. Manuscript submitted to publisher.
Schmertmann, J.H. (2000). The No-Filter Factor of Safety Against Piping Through Sands. In F. Silva & E.J. Kavazanijian (Eds.), *Judgement and Innovation* (pp. 65–133). American Society of Civil Engineers.
Sellmeijer, H., López, J., Cruz, D., van Beek, V.M. & Knoeff, H. (2011). Fine-tuning of the backward erosion piping model through small-scale , medium-scale and IJkdijk experiments. *European Journal of Environmental and Civil Engineering*, *15*(8), 1139–1154. https://doi.org/10.3166/EJECE.15.1139-1154
Sellmeijer, J.B. (1988). *On the mechanism of piping under impervious structures*. Delft University of Technology.
Sellmeijer, J.B. (2006). Numerical computation of seepage erosion below dams (piping). *International Conference on Scour and Erosion*.
TAW. (1999). *Technical Report on Sand Boils (Piping)*. Delft, The Netherlands.
Townsend, F., Schmertmann, J.H., Logan, T.J., Pietrus, T.J., & Wong, Y.W. (1981). *An Analytical and Experimental Investigation of a Quantitative Theory for Piping in Sand*. Gainesville, FLorida.
Turnbull, W.J., & Mansur, C.I. (1961). Investigation of underseepage- Mississippi River Levees. *ASCE Transactions*.
USACE. (1956). Investigation of Underseepage, Mississippi River Levees, Alton to Gale, IL. Vicksburg, MS: Waterways Experiment Station.
Van Beek, V., Bezuijen, A., Sellmeijer, J., & Barends, F.B.J. (2014). Initiation of backward erosion piping in uniform sands. *Géotechnique*, *64*(12), 927–941.
Van Beek, V., Knoeff, H., & Sellmeijer, H. (2011). Observations on the process of backward erosion piping in small-, medium- and fullscale experiments. *European Journal of Environmental and Civil Engineering*, *15*(8), 1115–1137. https://doi.org/10.3166/ejece.15.1115-1137
Van Beek, V.M. (2015). *Backward Erosion Piping: Initiation and Progression*. Technische Universiteit Delft. https://doi.org/10.1007/s13398-014-0173-7.2
Van Beek, V.M., Luijendijk, M. S., Knoeff, J. G., & Barends, F. B. J. (2009). Influence of relative density on the piping process - Small- scale experiments.
Van Beek, V.M., Robbins, B.A., Hoffmans, G., Bezuijen, A., van Rhijn, L. (2017). Use of incipient motion data for backward erosion piping modeling. Manuscript submitted to publisher.
Van Esch, J.M., Teunissen, J.A.M., & Stolle, D. (2013). Modeling transient groundwater flow under dikes and dams for stability assesment. In *3rd International Symposium on Computational Geomechanics (ComGeo III)* (p. 9).
Vandenboer, K., van Beek, V., & Bezuijen, A. (2014). 3D finite element method (FEM) simulation of groundwater flow during backward erosion piping. *Frontiers of Structural and Civil Engineering*, *8*(2), 160–166. https://doi.org/10.1007/s11709-014-0257-7
Weijers, J., & Sellmeijer, J. (1993). A new model to deal with the piping mechanism. *Filters in Geotechnical and Hydraulic Engineering*, 349–355. Retrieved from http://scholar.google.com/scholar?hl=en&btnG=Search&q=intitle:A+new+model+to+deal+with+the+piping+mechanism#0
White, C.M. (1940). The Equilibrium of Grains on the Bed of a Stream. *Proceedings of the Royal Society A: Mathematical, Physical and Engineering Sciences*, *174*(958), 322–338. https://doi.org/10.1098/rspa.1940.0023
White, S. (1970). Plane bed thresholds of fine grained sediments. *Nature*, *228*, 152–153. Retrieved from

http://adsabs.harvard.edu/abs/1970Natur.228..152W
Yalin, M., & Karahan, E. (1979). Inception of sediment transport. *Journal of the Hydraulics Division*. Retrieved from http://cedb.asce.org/cgi/WWWdisplay.cgi?5014975